STRUCTURAL CHARACTERIZATION OF LIGNIN FROM NATIVE, KRAFT AND SODA-AQ PULPING OF *PENNISETUM SINESE ROXB. (P. SINESE)*

JIACHUAN CHEN,[*] FENG SHEN,[*] GAOJIN LYU,[*] GUIHUA YANG,[*] NAN LU[*] and CHANGQING HU[**]

[*]*Key Laboratory of Pulp and Paper Science and Technology of the Ministry of Education, Qilu University of Technology, Jinan, Shandong 250353, P.R. China*
[**]*Zhanjiang Chenming Pulp and Paper Co., Ltd., Guangzhou, Guangdong 524000, P.R. China*
✉ *Corresponding author: Gaojin Lyu, gaojinlv@qlu.edu.cn*

Received February 23, 2017

Lignins isolated from native *Pennisetum sinese Roxb.* (*P. sinese*) and black liquor from kraft and soda-AQ pulping processes were characterized and compared by the analysis of alkaline nitrobenzene oxidation/HPLC, FT-IR, ^{31}P-NMR and 2D-HSQC NMR. The purpose was to distinguish lignins' structural differences and explore the mechanisms in the pulping process. Major functional groups and lignin linkages (*β*-O-4', *β-β*', *β*-5' *etc*.) were identified, and the structure of *P. sinese* lignin was described as a typical GSH-type lignin. Enzymatic mild acidolysis lignin (EMAL) contained a predominant proportion of syringyl units and guaiacyl units (syringyl/guaiacyl ratio of 1.2-1.4), along with a large amount of associated *p*-coumarates and ferulates. Soda-AQL and KL showed a significant decrease in *β*-O-4' linkages, while *β-β*' and *β*-5' linkages appeared to be especially resistant during the pulping process. In addition, an obvious decrease in aliphatic hydroxyl and a significant increase in total phenolic hydroxyl were noted after kraft and soda-AQ pulping.

Keywords: lignin, EMAL, *P. sinese*, ^{31}P-NMR, 2D-HSQC NMR

INTRODUCTION

Lignocellulosic biomass, made up of cellulose, hemicelluloses and lignin, is an excellent material for biofuels production due to its abundant quantity, renewability and carbon neutrality.[1,2] The biorefinery is a natural concept emerging from the use of biomass feedstocks, such as woods and grasses, agricultural residuals and energy crops in lieu of petroleum to address global warming and depletion of fossil fuels.[3]

Lignin is a major source of renewable aromatic chemicals. Soda-AQ and kraft pulping are widely used in the pulp and paper industry to manufacture fibers from grasses and woods, but these processes return copious amounts of waste lignin. The recently developed and commercialized LignoBoost™ technology offers the recovery of lignin from black liquors to provide a green approach for lignin isolation.[4-6] A lot of alternative utilizations for lignin have been investigated, including as all-purpose antioxidants, binders and dispersants[1,7,8] or as a bio-based alternative to oil and fossil fuels and raw material for synthesis of novel high-molecular polymers.[6,9]

Energy crops are an attractive alternative for the production of pulp and paper, textiles, bioethanol and biofuels due to their high productivity and low input for cultivation.[10] *P. sinese*, as one of the energy crops, is highly productive, but has been largely underexploited. It is a monocot C_4 perennial grass that is a hybrid of *Pennisetum purpureum* and *Pennisetum americanum*. It is versatile and adaptable and can consequently grow and thrive in a variety of harsh climates. Its high productivity (~40 t ha^{-1} y^{-1}) allows it to be harvested 3-4 times per year, which recommends it as a potential lignocellulosic feedstock.[11]

Lignin, located in the plant cell wall with cellulose and hemicelluloses, is a complex macromolecule mainly composed of three monomers: *p*-hydroxyphenyl (H), guaiacyl (G) and syringyl (S). Its structure is characterized by a variety of functional groups and over 10 diverse chemical linkages that vary greatly among species and individuals, and even within the tissues of the same plant.[7,12] Located in the plant cell wall, lignin plays a decisive role in the manipulation of the

lignocellulosic matrix.[13] However, lignin fractions are extremely variable, which has been conjectured to hinder the accessibility of biomass polysaccharides to enzymatic hydrolysis, thus delaying the biorefinery evolution.[14] In order to overcome biomass recalcitrance and facilitate widespread applications of lignin, understanding the structural characteristics of lignin from black liquors is crucial.[15]

It is a pre-requisite to extract and isolate representative lignin from the plant cell wall and black liquor before lignin is characterized. A lot of research work about the structural elucidation of lignin has been explored. Milled wood lignin (MWL), obtained by Björkman,[16,17] has been the standard bearer. Next, cellulolytic enzyme lignin (CEL) has been considered as a method to obtain lignin with a higher yield and less degradation, and its structure is similar to that of MWL.[18-20] Moreover, enzymatic mild acidolysis lignin (EMAL) is purer than MWL and CEL.[20] Precipitation of lignin from pulping black liquor using inorganic acids has already been proposed.[21-23]

Presently, the literature reports structural differences between *P. sinese* native and residual lignins, but there is less research work on the structural characterization of the lignin isolated from *P. sinese*.[2,11] Therefore, it is quite necessary to isolate lignins from original *P. sinese* and black liquor produced from kraft and soda-AQ pulping processes, and then characterize and compare them by an array of analytical techniques. It may be beneficial to use *P. sinese* to produce value-added products.

EXPERIMENTAL

Materials

One-year old *P. sinese* was obtained from Guangdong Province, China. Prior to chemical composition analysis, the chips were dried at 60 °C for 16 h in an oven and were ground to pass a 40 mesh screen (≤0.45 mm). The powders were extracted with a mixture of benzene and 95% ethanol (2:1, v/v) in a Soxhlet apparatus for 6 h to remove extractives. The chemical composition analysis of *P. sinese* was based on the methods developed by the National Renewable Energy Laboratory.[24]

Isolation and purification of enzymatic mild acidolysis lignin (EMAL)

An amount of 40 g of extractive-free samples were ground in a MB-O planetary ball mill (CHUO Kagaku, Japan) at 300 rpm for 72 h using the procedure of Björkman.[25] The isolation of the EMAL was based on the method developed and modified by Wu and Guerra.[20,26,27] Ball-milled powders were treated by industrial cellulase (from Novozyme) with an activity of 10,000 units/mL carboxyl methyl cellulose. The enzymatic hydrolysis was carried out in a water bath shaker at biomass loading of 5%, pH of 4.5 (acetic acid-sodium acetate as buffer solution), and 45 °C for 48 h. Then, the crude enzymatic lignin was centrifuged and washed three times with 0.01 $mol \cdot L^{-1}$ hydrochloric acid (HCl), and freeze-dried.

Impure lignin (10 g) was suspended in 200 mL of a mixture of acidic dioxane and deionized water (85:15, v/v, 0.01M) and refluxed at 87 °C under nitrogen for 2 h. The mixture solution obtained was filtered and washed with the mixture of dioxane and deionized water (85:15, v/v) for 2-3 times. The filtrate solution was neutralized with sodium bicarbonate ($NaHCO_3$). The neutralized solution was then rotary evaporated at 40 °C until the ideal thick solution. The thick solution was dropped into excess acidified deionized water (pH 2.0), and then the precipitated lignin was centrifuged and freeze-dried. Finally, the obtained lignin was further washed with hexane and dried in vacuum oven at 40 °C. The yield of isolated EMAL was 23.2% based on the original lignin content.

Preparation of soda-AQ lignin and kraft lignin

Soda-AQ pulping was carried out under the following conditions: 14% NaOH, 0.05% AQ, liquor-to-samples ratio of 5:1 (mL/g), and pulping time of 2.5 h at 160 °C. Kraft pulping process was performed under the following conditions: NaOH of 14%, Na_2S of 18%, liquor-to-samples ratio of 5:1 (mL/g), and pulping time of 2.5 h at 160 °C. The Kappa numbers of the obtained soda-AQ and kraft pulps were 17.6 and 18.9, respectively. Residue lignin from black liquors was obtained by dilute acid precipitation[28,29] and purified by the method described in the literature.[20] The yields of the prepared Soda-AQL and KL were of 4.1 g and 4.3 g per 100 mL of black liquor, respectively.

Alkaline nitrobenzene oxidation/HPLC

The determination of the S/G ratio of lignin monomers was carried out by alkaline nitrobenzene oxidation (NBO), as modified by Dence *et al*.[30] and Ohra-Aho *et al*.[31] An amount of 0.2 g of lignin samples, 6 mL of 2 M NaOH solution, and 0.5 mL of nitrobenzene were taken into a stainless steel vessel and reacted for 2 h at 170 °C. Afterwards, the hot steel vessel was cooled with cold water. The mixture was filtered and extracted 3 times with

30 mL $CHCl_3$ to remove unreacted nitrobenzene and derived products. The aqueous phase was acidified with 2 M HCl solution to pH 1-2. The acidified solution was further extracted 3 times with 30 mL of $CHCl_3$ and 1 time with 30 mL of diethyl ether. The organic phase was dried by Na_2SO_4 and evaporated to dryness. The dried products were dissolved in 1 mL dioxane and were further identified and quantified by high performance liquid chromatography (HPLC) in a Shimadzu CEM-10A apparatus equipped with a UV-VIS detector and C-18 (250 mm × 4 mm, 5 μm) reverse phase analytical column at 280 nm. The mixture of acetonitrile and water (12:88, v/v), containing 0.1% phosphoric acid, was used as mobile phase at a flow rate of 1.2 mL/min. The column temperature was maintained at 30 °C. Aromatic monomers used as references for qualification and quantification included gallic acid, protocatechuic acid, *p*-hydroxybenzaldehyde, vanillic acid, syringic acid, *p*-hydroxybenzoic acid, vanillin, syringaldehyde, *p*-coumaric acid and ferulic acid.

FT-IR spectroscopy

FT-IR spectra of the lignin samples were recorded on a FT-IR spectrophotometer (VERTEX70, Bruker, Germany) over 4000-400 cm^{-1}, using a KBr disc containing 1% finely ground samples.

NMR spectroscopy

NMR spectra were recorded on a Bruker AV III 400 MHz NMR. For Quantitative ^{31}P-NMR, pyridine-d_5/$CDCl_3$ (1.6:1, v/v) was used as solvent, cyclohexanol as internal standard, chromium acetylacetonate as relaxation reagent and 2-chloro-4,4,5,5-tetramethyl-1,3,2-dioxaphospholane (TDMP) as phosphorylating reagent.[32-34] For acquisition of the 2D HSQC NMR spectra, the spectral widths were 5000 and 20000 Hz, and 50 mg of lignin was dissolved in 0.5 mL DMSO-d_6.[35]

RESULTS AND DISCUSSION

Composition analysis of *P. sinese* and isolated lignins

Composition analysis of *P. sinese* and isolated lignins was carried out and the results are listed in Table 1. As can be seen clearly, the main chemical components were cellulose, hemicelluloses and lignin, in which the lignin content of *P. sinese* was 20.1%. The carbohydrate components of *P. sinese* accounted for 65.26%, which mainly consisted of glucose (40.64%), xylose (21.47%) and arabinose (1.82%). The purity of EMAL (92.5%) was around 5% lower than those of the corresponding Soda-AQL and KL, indicating that the lignin samples isolated from *P. sinese* still contain a few associated carbohydrates and other non-lignin contaminants, such as lignin-carbohydrate linkages. Such interactions between lignin and carbohydrates impede the isolation of lignin in high purities.[9]

Comparison of nitrobenzene oxidation and determination of S/G

The monomer composition and S/G ratio of three isolated lignins were analyzed by alkaline nitrobenzene oxidation/HPLC and the results are listed in Table 2. As shown in Table 2, syringaldehyde and vanillin, which represent typical syringyl-(S) and guaiacyl-(G) units, were the two dominant products from alkaline NBO of grass lignin; followed by *p*-coumaric acid, ferulic acid and *p*-hydroxybenzaldehyde. Vanillic acid, syringic acid and *p*-hydroxybenzoic acid were minor constituents, whereas the yield of gallic acid and protocatechuic acid were negligible. This observation provides information about the composition of the original polymer. The predominant product, syringaldehyde, accounted for 31.2-43.3% of the total NBO products. Vanillin was the second major degradation product, which amounted to 25.3-30.6%. It could be seen that the contents of hydroxycinnamates (*p*-coumarate (PCA) and ferulate (FA)) in EMAL were higher than those in KL and Soda-AQL, which indicated the lignin-carbohydrate components (LCC) were unstable during the delignification process.[9] The ratio of syringyl to guaiacyl (S/G) was given in many studies as an index of the degradation of lignin. Specifically, the S/G ratio analyzed by the alkaline NBO method was found to correlate with the proportion of the condensed structures of lignin, *i.e.* more non-condensed alkyl-aryl ether linkages (*β*-O-4') resulted in higher S/G ratio.[36,37] Moreover, the *β*-aryl ether linkage in syringyl lignin was cleaved much more easily than that in guaiacyl lignin.[38]

Table 1
Chemical composition of *P. sinese* and isolated lignins

	Purity	Carbohydrates (%)					Total carbohydrates	AIL	ASL
	(%)	Arabinose	Galactose	Glucose	Xylose	Mannose	(%)	(%)	(%)
P. sinese	-	1.82	0.61	40.64	21.47	0.73	65.26	16.35	3.74
EMAL	92.5	0.42	0.27	0.91	5.75	0.25	7.50	87.32	5.18
Soda-AQL	97.5	0.11	-	0.41	1.98	-	2.50	93.36	4.14
KL	97.8	0.15	-	0.37	2.48	-	3.0	93.47	4.33

Table 2
Content (area %) of phenolic acids and aldehydes in the alkaline nitrobenzene oxidation products of EMAL, Soda-AQL and KL from *P. sinese*

Phenolic acids and aldehydes	Content of oxidation products (area %)		
	EMAL	Soda-AQL	KL
Gallic acid	0.67	0.84	0.65
Protocatechuic acid	0.21	-	0.24
p-Hydroxybenzoic acid	0.71	0.91	1.78
Vanillic acid	2.50	4.52	3.86
p-Hydroxybenzaldehyde	7.40	5.91	2.33
Vanillin	24.80	27.29	28.61
Syringic acid	4.75	5.25	6.26
Syringaldehyde	33.21	44.22	45.31
p-Coumaric acid	14.52	3.10	2.80
Ferulic acid	11.21	7.96	8.16
S/G*	1.40	1.56	1.59

*G – total amount of vanillin and vanillic acid, S – total amount of syringaldehyde and syringic acid

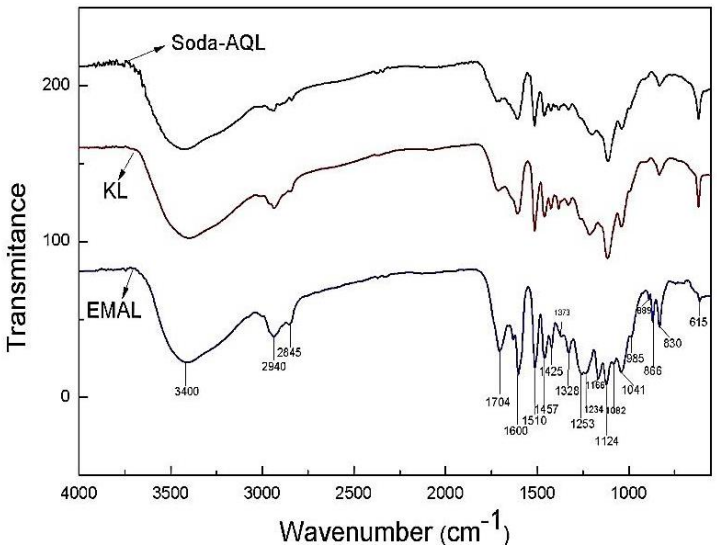

Figure 1: FT-IR spectra of the isolated lignins

In addition, it had been proposed that the *β*-O-4' bond was a dominant structure in lignin and highly related to the S/G ratio during the kraft pulping process.[39-41] In this work, the S/G molar ratio of EMAL was 1.40, whereas that of KL and Soda-AQL from black liquor showed a similar regularity of 1.56 and 1.59, respectively. The reason for the increase of S/G ratio was probably that more S-rich lignins were extracted from *P. sinese* under alkaline conditions.[9,31]

FT-IR analysis

FT-IR spectroscopy was used to examine the 3 types of lignins, and the absorption assignments were based on the literature.[35,42,43] As can be seen from the spectra of *P. sinese* EMAL, KL and Soda-AQL in Figure 1, the band at 3400 cm^{-1} was ascribed to the OH stretching of hydroxyl functional groups. The bands at 2941 and 2845 cm^{-1} were attributed to C-H stretching absorption bands, while the band at 1461 cm^{-1} was assigned to C-H asymmetric deformations. The absorbances at 1600, 1510 and 1420 cm^{-1} originated from aromatic skeleton vibrations. Moreover, the band at 1264 cm^{-1} identified with alkyl aryl ether bond represented guaiacyl (G) structures; the signals at 1120 and 1030 cm^{-1} associated with the presence of dialkyl ethers represented syringyl (S) structures; besides, the small band at 1232 cm^{-1} represented the *p*-hydroxyphenyl (H) unit. The FT-IR spectra therefore demonstrated that *P. sinese* EMAL was a typical GSH-type lignin. It should be noted that the structure of lignin extracted from black liquor changed; however, the characteristic bands of lignins from the two pulping processes were very similar.

Analysis of ^{31}P-NMR spectra

As known, phenolic OH plays an important role in lignin reactivity.[34] Quantitative ^{31}P-NMR of the three lignins was further recorded to investigate the phenolic hydroxyl group and *β*-aryl ether bond contents, and the results are presented in Table 3 and Figure 2. It was observed that the content of S-type phenolic hydroxyl groups in EMAL was lower than that of G-type OH, probably because most of the S-type lignin unit was involved in the formation of the *β*-O-4' linkages and only a slight amount of free S-OH could be detected;[9] as a result, the S/G ratio of EMAL was slightly lower. After kraft and soda-AQ pulping, the content of aliphatic OH decreased significantly, while an obvious increase in the total phenol hydroxyl concentration appeared. These were attributed to the cleavage of the *β* ether band and degradation.[36] It was also observed that the content of non-condensed S-OH and G-OH increased obviously as compared to that of condensed S-OH and G-OH structures in KL and Soda-AQL, which indicated that the cleavage of *β*-O-4' linkages appeared in the pulping process.[34,36] In addition, the content of the non-condensed H-OH was relatively stable during the pulping processes, while the -COOH content increased significantly, which probably contributed to the cleavage of the LCC linkages, and thus more glucuronic acid was released during the alkali pulping

process.[9] Additionally, the increase of the -COOH content was probably due to the oxidation of aliphatic OH, which could be reflected in the decreased aliphatic OH in KL and Soda-AQL.[44] Compared to EMAL, the structure features of KL and Soda-AQL were more similar.

Table 3
Quantification of functional groups in EMAL, KL and Soda-AQL from *P. sinese* by Quantitative ^{31}P-NMR

Functional groups	Shift δ (ppm)	Concentration (mmol/g)		
		EMAL	Soda-AQL	KL
Aliphatic-OH	150.0~145.0	3.96	2.70	1.29
Condensed S-OH	144.4~143.1	0.04	0.56	0.44
Non-condensed S-OH	143.1~142.4	0.17	1.79	1.21
Condensed G-OH	142.4~141.5	0.02	0.32	0.16
Non-condensed G-OH	140.0~138.8	0.36	1.36	0.85
Non-condensed H-OH	138.2~137.4	1.03	0.98	1.09
COOH	135.6~134.0	0.05	0.45	0.41
Total phenolic-OH	-	1.62	5.01	3.75
S/G ratio* (phenolic-OH)	-	0.55	1.40	1.63

*G – total amount of vanillin and vanillic acid, S – total amount of syringaldehyde and syringic acid

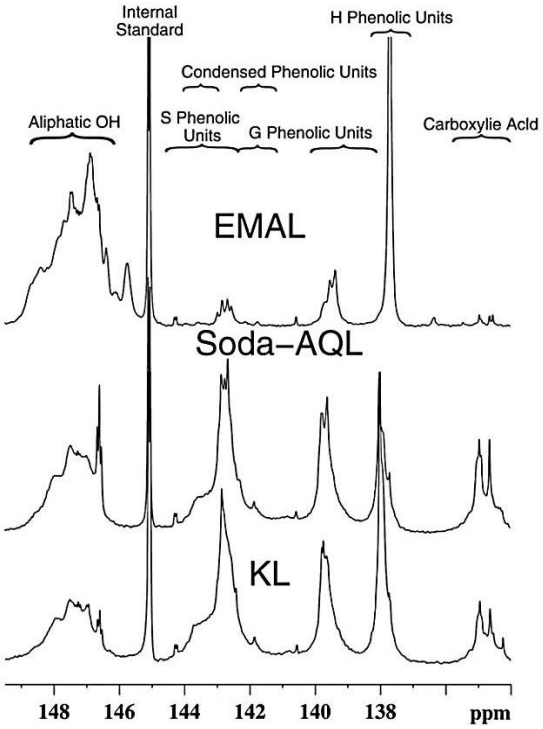

Figure 2: Quantitative ^{31}P-NMR of EMAL, KL and Soda-AQL from *P. sinese*

2D-HSQC spectra

2D-HSQC spectra could give more structural information about the lignins. The aliphatic and aromatic regions of the 2D-HSQC spectra of different lignins are shown in Figure 3. The peaks are assigned based on previous data and listed in Table 4. Accordingly, the main lignin substructures are depicted in Figure 4.[45,46] The side-chain region of the spectra revealed detailed information about the inter-unit linkages. The spectra showed prominent signals corresponding to β-O-4' aryl-ether linkages (substructures A and A'). The C_α-H_α correlations in β-O-4' substructures were located at δ_C/δ_H 72.0/4.70-4.90. Likewise, the C_β-H_β correlations were observed at δ_C/δ_H 83.5/4.35 and 86.0/4.12 for the β-O-4' structures linked to G and S units. The C_γ-H_γ correlations were observed at δ_C/δ_H 60.0/3.40 and 60.0/3.56 for the β-O-4' structures, partially superimposed on other signals. In addition, the C_γ-H_γ correlations in γ-acylated lignin units (A') were also observed at δ_C/δ_H 63.0/4.29.

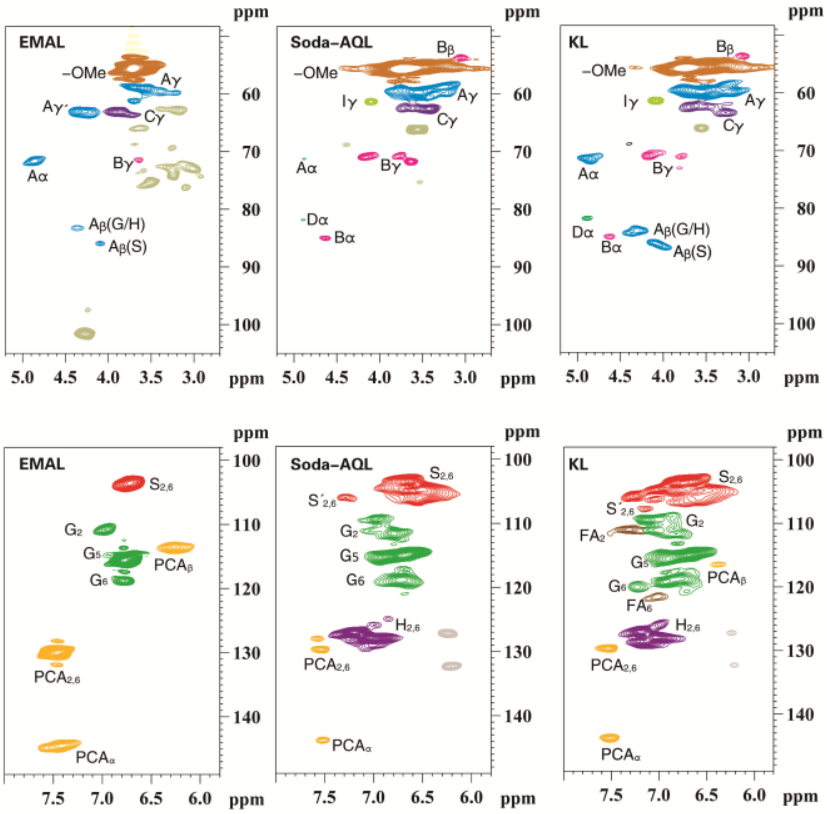

Figure 3: Aliphatic and aromatic regions of 2D-HQSC NMR spectra of EMAL, KL and Soda-AQL from *P. sinese*

Table 4
Assignments of lignin ^{13}C-^{1}H correlation signals in 2D-HSQC NMR spectra of EMAL, KL and Soda-AQL from *P. sinese*

Labels	δ_C/δ_H (ppm)	Assignment
B_β	54.0/3.12	C_β-H_β in *β-β*' (resinol) substructures (B)
-OMe	55.6/3.72	C-H in methoxyls (MeO)
A_γ	60.7/3.53	C_γ-H_γ in *β-O*-4' substructures (A)
I_γ	62.5/4.30	C_γ-H_γ in *p*-hydroxycinnamyl alcohol end groups (I)
A'_γ	63.0/4.11	C_γ-H_γ in *γ*-acetylated *β-O*-4' substructures (A'$_\gamma$)
C_γ	63.1/3.78	C_γ-H_γ in phenylcoumaran substructures (C)
B_γ	71.6/3.69	C_γ-H_γ in *β-β*' (resinol) substructures (B)
A_α	72.0/4.89	C_α-H_α in *β-O*-4' substructures linked to a S unit (A)
A_β (S)	84.9/4.12	C_β-H_β in *β-O*-4' substructures linked to a S unit (A)
A_β (G/H)	83.5/4.45	C_β-H_β in *β-O*-4' substructures linked to a G and H units (A)
$S_{2,6}$	104.3/6.72	$C_{2,6}$- $H_{2,6}$ in syringyl units (S)
G_2	111.3/6.96	C_2-H_2 in guaiacyl units (G)
FA_2	111.0/7.32	C_2-H_2 in ferulic acid units (FA)
PCA_β	114.3/6.25	C_8-H_8 in *p*-coumaric acid (PCA)
G_5	115.3/6.76	C_5-H_5 in guaiacyl units (G)
	114.0/6.67	
$PCA_{3,5}$	115.5/6.77	C_3-H_3 and C_5-H_5 in p-coumarate
FA_6	123.0/7.10	C_6-H_6 in ferulic acid units (FA)
$H_{2,6}$	128.0/7.23	$C_{2,6}$-$H_{2,6}$ in *p*-hydroxyphenyl units (H)
G_6	119.0/6.89	C_6-H_6 in guaiacyl units (G)
$PCA_{2,6}$	130.3/7.42	$C_{2,6}$-$H_{2,6}$ in *p*-coumaric acid (PCA)
PCA_α	144.4/7.39	C_7-H_7 in *p*-coumaric acid (PCA)

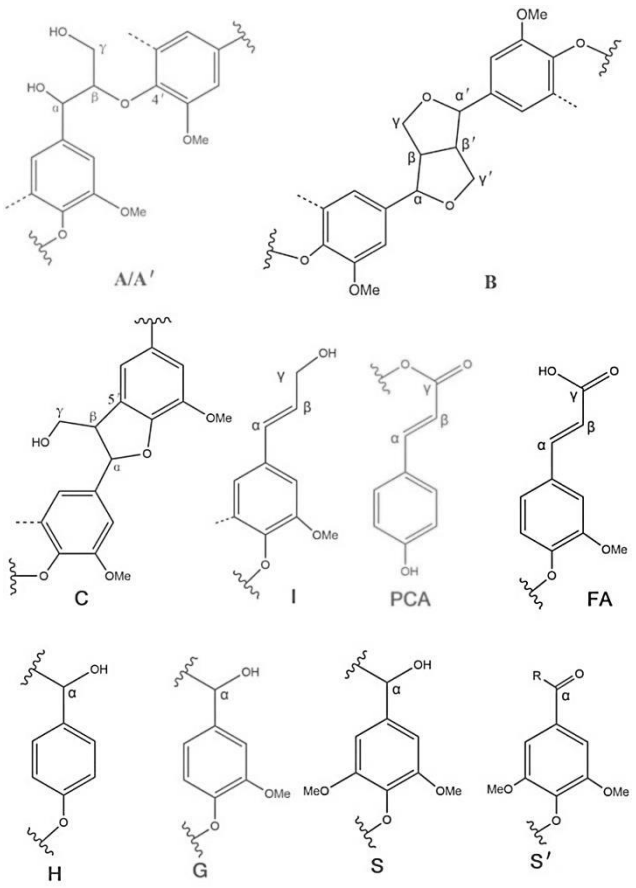

Figure 4: Main structures present in EMAL, KL and Soda-AQL from *P. sinese*: (A) *β*-O-4' linkages; (A') *β*-O-4' linkages with acetylated *γ*-carbon; (B) resinol structures formed by *β*-*β*', *α*-O-*γ*' and *γ*-O-*α*' linkages; (C) phenylcoumarance structures formed by *β*-5' and *α*-O-4' linkages; (I) *p*-hydroxycinnamyl alcohol end-groups; (PCA) *p*-coumarate units; (FA) ferulate units; (H) *p*-hydroxyphenyl units; (G) guaiacyl units; (S) syringyl units; (S') oxidized syringyl units bearing a carbonyl groups at C_{α}

Moreover, signals for resinol (*β*-*β*', substructures B) were also found in the spectra. The signal of C_{α}-H_{α} (δ_C/δ_H) was at approximately 83.6/4.81, while the signals of C_{γ}-H_{γ} (δ_C/δ_H) were observed at 71.6/3.69. The signal of C_{γ}-H_{γ} (δ_C/δ_H) from phenylcoumaran (*β*-5', substructures C) was also detected at 63.5/3.78, which partially overlapped with the signals of C_5-H_5 from xylans. Furthermore, the signal located at 62.5/4.15 (δ_C/δ_H) was assigned to the C_{γ}-H_{γ} correlation of *p*-hydroxycinnamyl alcohol end groups (I). Compared to the EMAL spectrum, the signal intensity of *β*-*β*' and *β*-5' cross peaks in KL and Soda-AQL increased, and some ether substructures were detected during the alkaline reaction.

In the aromatic region of the 2D-HSQC spectra of the lignin samples, signals originating from G units, S units, *p*-hydroxycinnamyl (H) unit, *p*-coumarates (PCA) and ferulates (FA) were obviously distinguished. The S-lignin unit showed a prominent signal for the $C_{2,6}$-$H_{2,6}$ (δ_C/δ_H) correlations at 103.6/6.69, while the signals for the C_{α}-oxidized S-units (S') were found at 106.3/7.19 (δ_C/δ_H). Conversely, the G-units showed different correlations: C_2-H_2 (δ_C/δ_H, 111.0/6.96), C_5-H_5 (δ_C/δ_H, 115.4/6.75), and C_6-H_6 (δ_C/δ_H, 118.9/6.77). Cross-signals corresponding to $C_{2,6}$-$H_{2,6}$ correlations of H lignin units were detected at 128.0/7.23. Signals corresponding to *p*-coumarates structures (PCA) were observed in the spectra of the lignin fractions. Signals corresponding to the $C_{2,6}$-$H_{2,6}$ and $C_{3,5}$-$H_{3,5}$ were noted at 130.3/7.42 (δ_C/δ_H) and 115.4/6.77 (δ_C/δ_H), and signals for the correlations of the unsaturated C_{α}-H_{α} at 144.4/7.39 (δ_C/δ_H) and C_{β}-H_{β} at 114.3/6.25 (δ_C/δ_H) of the *p*-coumarate unit were observed in this region of the HSQC spectra.

Table 5
Substructure contents of EMAL, KL and Soda-AQL from *P. sinese* by Quantitative 2D-HSQC spectra

Linkages (%)*	EMAL	Soda-AQL	KL
β-O-4' substructures (A/A')	84.4	35.1	41.4
β-*β*' resinol substructures(B)	9.9	49.8	44.8
β-5' phenylcoumaran substructures (C)	5.7	15.1	13.8
S/G ratio	1.25	1.65	1.66

*Per 100 aromatic units and expressed as a percentage of the total linkage considered

Relative abundances of the main lignin inter-unit linkages and the S/G ratio calculated from the 2D HSQC spectra, based on previous work,[45] are shown in Table 5. As expected, the main substructures present in EMAL were *β*-O-4' ether linkages, which accounted for 84.4% of all inter-unit linkages, followed by *β*-*β*' resinol substructures (B), which involved 9.9% of all linkages, and minor amounts of *β*-5' phenylcoumaran substructures (C, 5.7%). Whereas *β*-O-4' alkyl-aryl ether linkages dramatically decreased during soda-AQ and kraft pulping processes, the predominant inter-linkage changed to *β*-*β*' resinol substructures (B), which seemed to be particularly resistant to soda-AQ and kraft pulping.[47] Furthermore, Soda-AQL and KL showed a similar percentage of *β*-5' linkages that ranged from 13.8% to 15.1%, much higher than that of EMAL. It indicated that the S/G ratio was important to elucidate the lignin isolation and delignification process.[48,49] In the present work, the EMAL of the native sample *P. sinese* had an S/G molar ratio of approximately 1.25, according to the HSQC spectra, which was lower than that of alkaline nitrobenzene oxidation (1.40). Del Rio *et al*. showed a similar lignin composition in the cortex and pith of elephant grass, with an S/G ratio around 1.30.[2] It has been generally considered that the S/G ratio obtained from NMR results is more accurate, since NMR can detect all the structural information of lignin, both the condensed and non-condensed parts.[50,51] In contrast, the nitrobenzene oxidation method only detects the S/G of releasable monomers, such as syringaldehyde, syringic acid, vanillin and vanillic acid *etc*. from the oxidative cleavage of condensed structures of lignin.[36,37] It was also found that the S/G ratios of Soda-AQL and KL increased to 1.65 after pulping. It was noted that alkaline pulping had a significant influence on the delignification of lignin. The EMAL displayed a predominance of the aryl ether *β*-O-4' linkages, which mainly consist of abundant S-type units. The amount of *β*-O-4' linkages seemed to decrease dramatically, which was probably related to the delignification of the alkaline pulping process.

CONCLUSION

The structure of *P. sinese* lignin was typical of GSH-type, with predominant syringyl and guaiacyl units. The original EMAL contained a syringyl/guaiacyl ratio of 1.2-1.4 and a large amount of associated *p*-coumarates and ferulates. For the lignins of black liquors from soda-AQ and kraft pulping processes, respectively, the analysis of 2D-HSQC and ^{31}P NMR demonstrated that, compared to the original EMAL, *β*-O-4' linkages were extensively degraded and broken during the pulping process, and *β*-*β*' and *β*-5' linkages were formed and appeared to be especially resistant to the pulping process. Moreover, an obvious decrease in aliphatic OH and a significant increase of the total phenol hydroxyl concentration were attributed to the cleavage and degradation of *β*-*O*-4' substructures.

ACKNOWLEDGEMENT: The authors are grateful for the financial support from the National Natural Science Foundation of China (Grants No. 31770630, 31470602, 31670590, 31670595), Major Science and Technology Projects of Shandong Province (No. 2014ZZCX09101, 2015ZDZX09002), and Taishan Scholars Project Special Funds.

REFERENCES

1 X. P. Peng, S. L. Sun, J. L. Wen, W.-L. Yin and R. C. Sun, *Fuel*, **134**, 485 (2014).
2 J. C. del Río, P. Prinsen, J. Rencoret, L. Nieto, J. Jiménez-Barbero *et al*., *J. Agric. Food Chem*., **60**, 3619 (2012).
3 M. E. Himmel, D. Shi-You, D. K. Johnson, W. S. Adney, M. R. Nimlos *et al*., *Science*, **315**, 804 (2007).
4 M. A. Khan, S. M. Ashraf and V. P. Malhotra, *J. Appl. Polym. Sci*., **92**, 3514 (2004).

[5] A. Tejado, C. Pena, J. Labidi, J. Echeverria and I. Mondragon, *Bioresour. Technol.*, **98**, 1655 (2007).
[6] M. Wang, M. Leitch and C. C. Xu, *Eur. Polym. J.*, **45**, 3380 (2009).
[7] N.-E. El Mansouri and J. Salvadó, *Ind. Crop. Prod.*, **24**, 8 (2006).
[8] S. Laurichesse and L. Avérous, *Prog. Polym. Sci.*, **39**, 1266 (2014).
[9] J.-L. Wen, S.-L. Sun, T.-Q. Yuan and R.-C. Sun, *Green Chem.*, **17**, 1589 (2015).
[10] T. You, L. Zhang, S. Guo, L. Shao and X. Feng, *J. Agric. Food Chem.*, **63**, 10747 (2015).
[11] Q.-L. Lu, L.-R. Tang, S. Wang, B. Huang, Y.-D. Chen *et al.*, *Biomass Bioenerg.*, **70**, 267 (2014).
[12] S. N. Sun, T. Q. Yuan, M. F. Li, X. F. Cao, F. Xu *et al.*, *Cellulose Chem. Technol.*, **46**, 165 (2012).
[13] S. Nanayakkara, A. F. Patti and K. Saito, *Green Chem.*, **16**, 1897 (2014).
[14] K. Sanderson, *Nature*, **474**, S12 (2011).
[15] F. Tran, C. S. Lancefield, P. Kamer, T. Lebl and N. Westwood, *Green Chem.*, **17**, 244 (2015).
[16] A. Björkman, *Nature*, **174**, 1057 (1954).
[17] A. Björkman, *Svensk Papperstidn.*, **59**, 477 (1956).
[18] H.-M. Chang, E. B. Cowling and W. Brown, *Holzforschung*, **29**, 153 (1975).
[19] Z. Hu, T.-F. Yeh, H.-M. Chang, Y. Matsumoto and J. F. Kadla, *Holzforschung*, **60**, 389 (2006).
[20] S. Wu and D. Argyropoulos, *J. Pulp Pap. Sci.*, **29**, 235 (2003).
[21] R. Sun, J. Tomkinson and J. Bolton, *Polym. Degrad. Stabil.*, **63**, 195 (1999).
[22] H. A. Khalil, M. Marliana and T. Alshammari, *Bioresources*, **6**, 5206 (2011).
[23] S. Hattalli, A. Benaboura, F. Ham-Pichavant, A. Nourmamode and A. Castellan, *Polym. Degrad. Stabil.*, **76**, 259 (2002).
[24] A. Sluiter, B. Hames, R. Ruiz, C. Scarlata, J. Sluiter *et al.*, Technical Report for Laboratory Analytical Procedure (LAP), NREL, Golden, CO, USA, (2010).
[25] A. Björkman, *Svensk Papperstidn.*, **59**, 477 (1956).
[26] A. Guerra, I. Filpponen, L. A. Lucia and D. S. Argyropoulos, *J. Agric. Food Chem.*, **54**, 9696 (2006).
[27] A. Guerra, I. Filpponen, L. A. Lucia, C. Saquing, S. Baumberger *et al.*, *J. Agric. Food Chem.*, **54**, 5939 (2006).
[28] R. Sun and J. Tomkinson, *Sep. Purif. Technol.*, **24**, 529 (2001).
[29] T.-Q. Yuan, J. He, F. Xu and R.-C. Sun, *Polym. Degrad. Stabil.*, **94**, 1142 (2009).
[30] C. W. Dence, in "Methods in Lignin Chemistry", edited by S. Y. Lin and C. W. Dence, Springer, 1992, pp. 33-61.
[31] T. Ohra-Aho, F. J. B. Gomes, J. L. Colodette and T. Tamminen, *J. Anal. Appl. Pyrol.*, **101**, 166 (2013).
[32] D. Argyropoulos, *Res. Chem. Intermed.*, **21**, 373 (1995).
[33] D. S. Argyropoulos, *J. Agric. Food Chem.*, **14**, 45 (1994).
[34] A. Granata and D. S. Argyropoulos, *J. Agric. Food Chem.*, **43**, 1538 (1995).
[35] J.-L. Wen, S.-L. Sun, B.-L. Xue and R.-C. Sun, *Materials*, **6**, 359 (2013).
[36] P. Prinsen, J. Rencoret, A. Gutiérrez, T. Liitiä, T. Tamminen *et al.*, *Ind. Eng. Chem. Res.*, **52**, 15702 (2013).
[37] H. Yang, Y. Xie, X. Zheng, Y. Pu, F. Huang *et al.*, *Bioresour. Technol.*, **207**, 361 (2016).
[38] Y. Tsutsumi, R. Kondo, K. Sakai and H. Imamura, *Holzforschung*, **49**, 423 (1995).
[39] D. Collins, C. Pilotti and A. Wallis, *Appita J.*, **43**, 193 (1990).
[40] P. C. Pinto, D. V. Evtuguin and C. P. Neto, *Ind. Eng. Chem. Res.*, **44**, 9777 (2005).
[41] S. K. Bose, R. C. Francis, M. Govender, T. Bush and A. Spark, *Bioresour. Technol.*, **100**, 1628 (2009).
[42] O. Faix, *Holzforschung*, **45**, 21 (1991).
[43] D. Fengel and X. Shao, *Wood Sci. Technol.*, **19**, 131 (1985).
[44] P. M. Froass, A. J. Ragauskas and J. E. Jiang, *J. Wood Chem. Technol.*, **16**, 347 (1996).
[45] J. C. del Río, P. Prinsen, J. Rencoret, L. Nieto, J. Jiménez-Barbero *et al.*, *J. Agric. Food Chem.*, **60**, 3619 (2012).
[46] J. Rencoret, P. Prinsen, A. Gutiérrez, Á. T. Martínez and J. C. del Río, *J. Agric. Food Chem.*, **63**, 603 (2015).
[47] H. Yang, X. Zheng, L. Yao and Y. Xie, *Bioresources*, **9**, 176 (2013).
[48] C. Fernández-Costas, S. Gouveia, M. A. Sanromán and D. Moldes, *Biomass Bioenerg.*, **63**, 156 (2014).
[49] A. Guerra, J. P. Elissetche, M. Norambuena, J. Freer, S. Valenzuela, *et al.*, *Ind. Eng. Chem. Res.*, **47**, 8542 (2008).
[50] R.Vanhome, J. Ralph, T. Akiyama, F.-C. Lu, J. Rencoret *et al.*, *Plant J.*, **64**, 885 (2010).
[51] D. Y. Min, H. Jameel, H. M. Chang, L. Lucia, Z. G. Wang *et al.*, *RSC Adv.*, **4**, 10845 (2014).